A Study of Microstructural Changes During Dehydration of Hydrolytically Degraded Poly(glycolic acid)

E. KING and R. E. CAMERON*

Department of Materials Science and Metallurgy,

University of Cambridge, Cambridge, England.

SYNOPSIS

The effect of dehydration on the microstructure of hydrolytically degraded, unoriented semi-crystalline poly(glycolic acid), PGA, was examined using environmental scanning electron microscopy (ESEM), thermogravimetric analysis (TGA) and simultaneous small and wide angle x-ray scattering (SAXS/WAXS). Samples were degraded in phosphate-buffered saline solution at 37°C and monitored during dehydration.

Few microstructural changes were observed on drying PGA after 1 hour degradation. However, on drying the hydrolytically damaged PGA, the lamellar repeat distance decreased as crystal lamellae collapsed together. The SAXS intensity profile showed voids simultaneously opening. Cracks became visible at the surface and the crystallites became more strained. The changes in surface microstructure on dehydration were found to be dependent on both the extent of hydrolytic attack and on the rate of removal of water.

Significant differences in microstructure and degree of hydration were observed between degraded PGA analysed wet, after freeze-drying and after vacuum-drying. These findings indicate the importance of sample preparation in the study of degradable materials.

 CCC 1022-1360/98/$ 10.00

INTRODUCTION

Poly(hydroxy acid)s are an important class of biodegradable polymers for biomedical applications due to their biocompatibility and their physiologically tolerable degradation products. Poly(glycolic acid), PGA, has been manufactured as a synthetic absorbable suture material and its success has led to its development for other medical applications, such as implants, vascular grafts, artificial skin grafts and drug release systems [1].

PGA is the simplest linear aliphatic polyester. The hydrophilic nature of the ester bond allows the polymer to be hydrolytically degraded by body fluids. It is a semi-crystalline thermoplastic with a high melting point of 224-227°C [2] and a glass transition temperature of around 37°C [3]. It has a very low solubility in most organic solvents [4] and this limits available processing techniques. The unit cell contains two molecular chains in a planar zig-zag conformation within an orthorhombic unit cell [5].

In an earlier study [6], we reported data from fully hydrated samples degraded PGA, analysed immediately after removal from the buffer solution. The changes in microstructure due to the hydrolytic attack were observed using simultaneous SAXS/WAXS and UV spectrophotometry. During degradation, the crystal density and lateral extent of the crystal lamellae remained constant. More dramatic changes were seen in the amorphous phase. Sharp increases in the crystallinity, the amount of glycolic acid in the buffer solution and in the density difference between the crystal lamellae and the layers separating them indicated a loss of amorphous material that levelled off after 30 days. The lamellar repeat distance fell from around 95Å to 80Å in the first 20 days before slowly rising again towards its initial value, changes that might be interpreted as reflecting a two stage loss of amorphous material, in which highly coiled loops and tie chains are degraded faster than taut tie chains. Changes in the osmotic potential of the water in the changing chemical environment in the degrading polymer are also likely to affect the swelling and hence the lamellar repeat.

Full characterisation of hydrolytically degraded polymers usually requires sample dehydration. Dehydration prevents further hydrolytic attack and allows concise structural analysis, such as thermal analysis and electron microscopy. The dehydration of degraded polymer, however, can result in additional structural damage. Environmental Scanning Electron Microscope (ESEM) images of degraded polyanhydride microspheres show that as moisture is removed, cracks form and propagate through the initially smooth sample surface [7].

Voided microstructures have been reported in several degraded and dried polymers. Ginde and Gupta [8], for example, studied surface features of degraded PGA pellets and fibres that were dried before analysis in a vacuum desiccator filled with anhydrous calcium sulphate They reported greater microcrack formation on the surface of pellets compared to the fibres. A recent study of PGA and PGA-co-poly(trimethylene carbonate) sutures also revealed surface cracks in degraded and dried samples [9]. These features were not observed in similarly treated injection moulded PGA disks. It was hypothesised that the surface cracks in the sutures were formed on degradation by continual alleviation of internal stresses generated by the drawing process. The absence of cracks in the disk was thought to be a consequence of a much lower degree of internal stress from processing. Since the samples were both degraded and dried, the effects of degradation and dehydration were not separated in these studies.

The relationships between degradation, dehydration and morphological change are clearly of importance if the results from dehydrated samples are to be correctly interpreted.

We present a study of the effect of drying on microstructure of hydrolytically degraded unoriented plates of semi-crystalline PGA. Simultaneous small and wide angle X-ray scattering (SAXS/WAXS) was used to monitor the morphological changes associated with water removal. TGA was used to investigate the effect of drying technique on the water

content. ESEM was employed to observe the effects of the water extraction on the surface features. Finally, a comparison was made between freeze dried, vacuum dried samples and wet samples.

EXPERIMENTAL

Materials. Pellets of PGA, with an inherent viscosity of 1.33 dl/g, were obtained from Medisorb Technologies International of Ohio. Plates 1 cm x 4 cm were formed by melting 0.8 g PGA at 230°C in a copper mould with a PTFE coated aluminium base, then crystallising at 160°C. Phosphate-buffered saline solution, pH = 7.4, from Sigma-Aldrich Company was made up with distilled water and 1% penicillin-streptomycin antibiotic solution, from Sigma-Aldrich Company was added. All the experimental apparatus was autoclaved for 30 minutes prior to use.

Plates of PGA were immersed in 50ml buffer solution at 37°C. After a predetermined period of time, the plates were removed from the buffer solution and either immediately analysed or dried using one of the following techniques.

Vacuum drying was performed by placing the samples in a vacuum oven at room temperature at 1 bar for a predetermined time. Desiccation was performed by placing the samples in a vacuum desiccator filled with anhydrous calcium sulphate at room temperature for a predetermined time. Freeze-drying was performed at Pfizer Central Research Laboratories by Dr J. Richardson and Mrs J. Woods. The samples were frozen in liquid nitrogen, then placed on a pre-cooled shelf in the freeze-drier at -40°C for 4 hours until total equilibrium was achieved. The temperature was increased to -30°C over 4 hours and maintained for 60 hours. Finally, the temperature was increased to 25°C over a period of 24 hours.

Time resolved SAXS/WAXS. Simultaneous SAXS/WAXS was performed on station 8.2 at the SRS Laboratory at Daresbury, UK. The SRS laboratory allows data to be obtained over short exposure times due to the high intensity of the synchrotron radiation. Ryan *et al* have described the experimental technique of SAXS/WAXS used to determine polymer structure [10].

The WAXS data was obtained using a curved knife-edge detector and the SAXS data was obtained using a quadrant detector located 3.5m from the sample position. The SAXS detector was calibrated using wet collagen and the WAXS using high density poly(ethylene). The SAXS data were divided by the detector response found by uniform illumination of the detector. Both WAXS and SAXS data were corrected for background scattering by subtracting the scattering from the straight through beam and for sample thickness and transmission by dividing by the signal from an ionisation chamber placed directly behind the sample. The 'tac' hole, an electronic function of the data collection, was removed.

Fully hydrated samples were placed directly into the beam in the DSC heating stage and heated at 10°C/min from room temperature to 80°C. This treatment removed most of the water. Data was collected at 30s intervals.

Single X-ray profiles were obtained at room temperature from degraded samples. Fully hydrated samples, freeze-dried samples and samples vacuum dried for 48 hours were exposed in the beam for 30s.

TGA. Four plates of PGA were degraded for 21 days as described above, then heated in a Perkin Elmer TGA from 30 - 100°C at 10°C/min. The four samples were removed from the buffer solution then analysed after different sample preparation techniques: a) fully hydrated, immediately after removal from the buffer solution, b) desiccated for 2 months, c) vacuum dried for 3 days and d) desiccated for 2 months followed by storage at 97% humidity for 2 hours.

ESEM. Two plates of PGA were degraded as above for 28 days and immediately observed by ESEM. The ESEM technique [11] allows direct imaging of wet and non-conducting materials without any sample preparation, such as drying or coating, and without the problematic specimen charging. This is achieved by use of a differential pumping system and a type of electron detector that allows the specimen chamber to contain water moisture. Thus, ESEM is capable of imaging wet samples and to monitor the change in surface features as water is removed.

A fully hydrated degraded PGA sample was placed in the microscope chamber at 0.5°C surrounded by buffer solution, and the chamber was slowly evacuated, maintaining the moisture within the sample. Finally, the chamber temperature was set to 4°C and with a water vapour pressure of 3 torr. At this stage the sample was still fully hydrated and the vapour pressure above it saturated. The temperature was increased slowly to 12°C so that the vapour pressure above the sample was no longer saturated and the effect of the removal of water was observed. This procedure was repeated for a second sample with the temperature rapidly increased to 12°C to observe the effect of the rate of water removal.

RESULTS

SAXS profiles during dehydration. Figure 1 shows the dynamic SAXS data obtained for the drying of PGA degraded for 1 hour, 28 days and 63 days. The intensities are in the same arbitrary units in each graph. The ultimate scattering intensity increases dramatically with degradation time as the scales on these graphs show. The profile from the sample degraded for 28 days shows an immediate increase in low angle intensity as the temperature is raised. In contrast, the profile from the sample degraded for 63 days shows such an increase only later stages of heating although the ultimate increase is much greater.

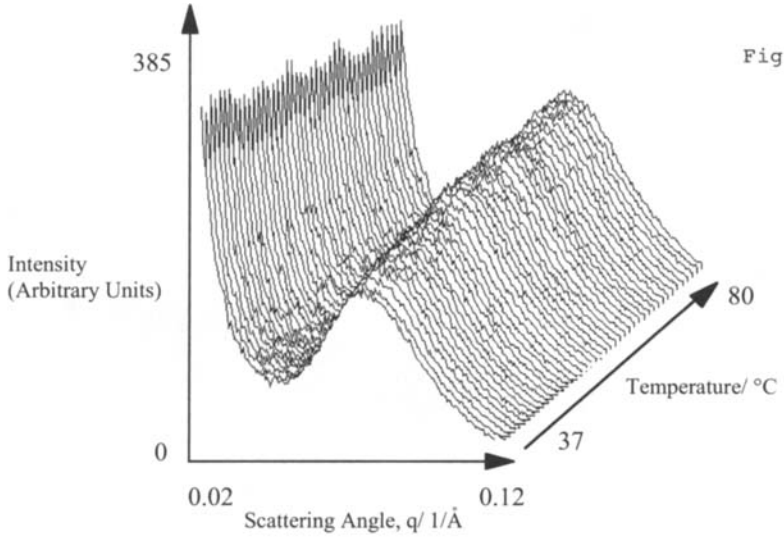

Fig. 1a

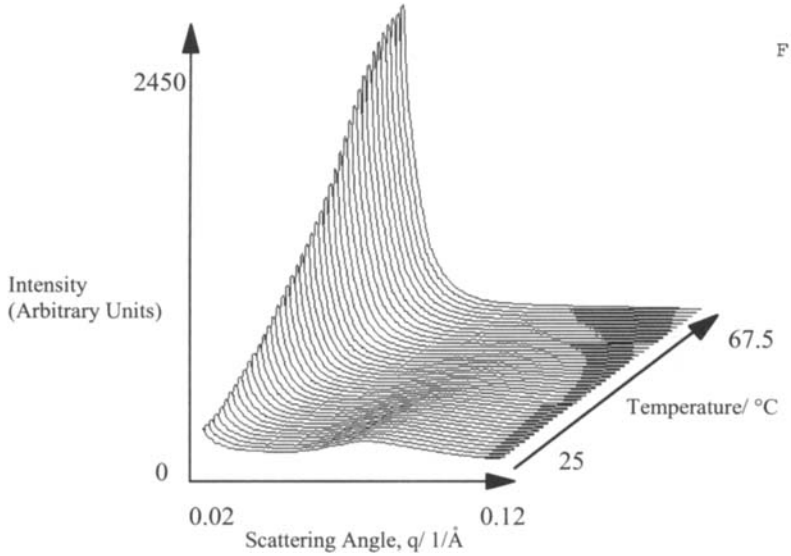

Fig. 1b

Figure 1: The dynamic SAXS intensity profiles for the drying of samples degraded for a) 1 hour b) 28 days and c) 63 days. The lamellar structure of the degraded samples is seen to collapse as voids open up, whereas the sample degraded for 1 hour is unaffected by the removal of water.

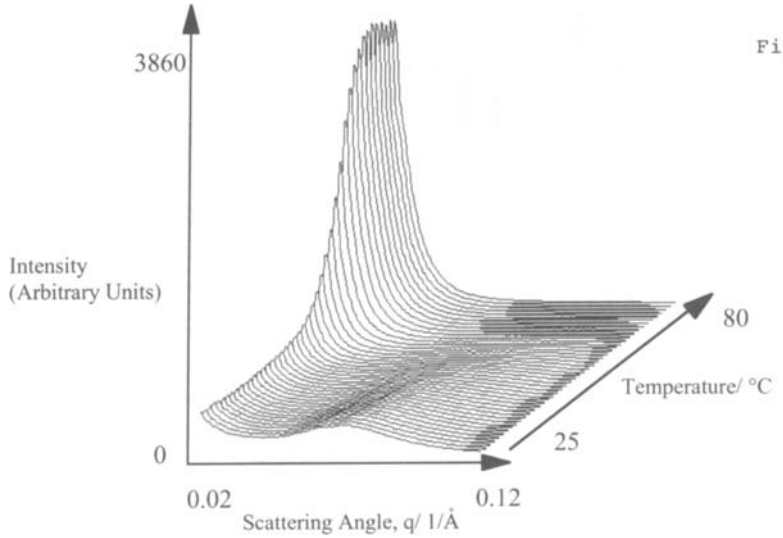

Fig. 1c

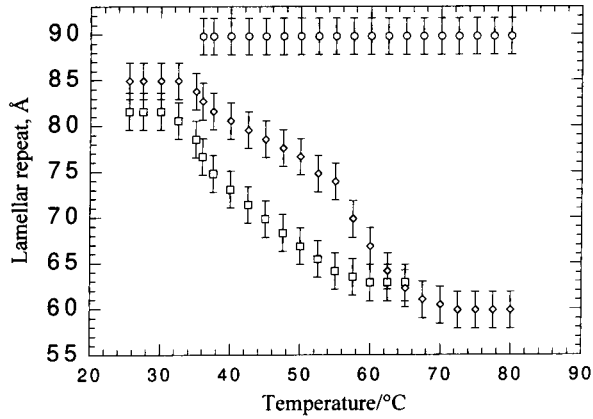

Figure 2: The total lamellar repeat distance plotted against temperature for samples degraded for 1 hour (circles), 28 days (squares) and 63 days (diamonds). The values are obtained by applying the Bragg equation to the peak positions of the Lorentz corrected SAXS intensity profiles. The value decreases on heating in the samples damaged by degradation.

An estimate of the effect of drying on the lamellar repeat distance may be obtained by applying the Bragg equation to the Lorentz corrected peak positions. The Lorentz correction is applied by multiplying the intensity by the square of the scattering vector, thereby converting the data from randomly oriented lamellar stacks to that from a single lamellar stack[12]. These repeat distances are shown in figure 2. The repeat distance for the sample degraded for 1 hour shows no change. In contrast, the value for the samples degraded for longer times show a clear fall during dehydration.

The invariant of a SAXS profile [12], Q, can be calculated using equation 1.

$$Q = \frac{1}{2\pi^2} \int_0^\infty q^2 I(q) dq \qquad (1)$$

The invariant is unaffected by the shape of the scattering entities, but is dependent on the change in electron density differences within the structure [13].

The change in the calculated invariant during dehydration of PGA degraded for 1 hour, 28 days and 63 days is shown in figure 3. The integration was performed between the limits of data collection. Since the intensities collected are in arbitrary units, the values obtained differ from the true invariant by a constant factor. Clearly the invariant is higher the longer the degradation time. The invariant for the sample degraded for 1 hour shows a slight rise with temperature. It falls however for the samples degraded for longer times.

WAXS profiles during dehydration. Figure 4 shows the WAXS data obtained during the dehydration of a sample of PGA degraded for 63 days. Similar curves were obtained for samples degraded for 28 days and 1 hour.

WAXS profiles were analysed using the peak fitting program 'fit', developed at the SRS, that fits curves to the crystal peaks and the amorphous halo. A Gaussian function was used to fit

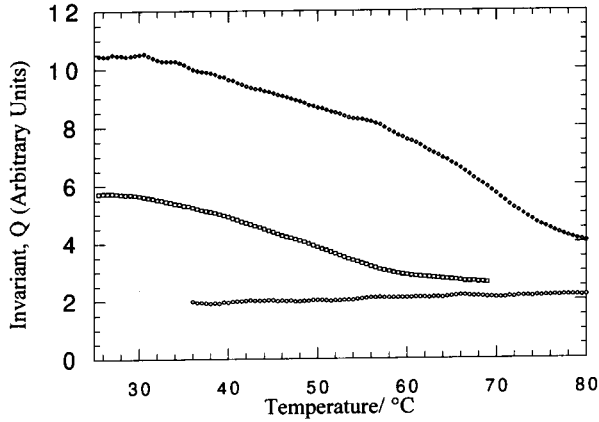

Figure 3: The invariant, Q, from the SAXS intensity profile, plotted against temperature for samples degraded for 1 hour (circles), 28 days (squares) and 63 days (diamonds). Since intensity is given in arbitrary units, the invariant is also obtained in arbitrary units, related to standard units by an unknown constant, k.

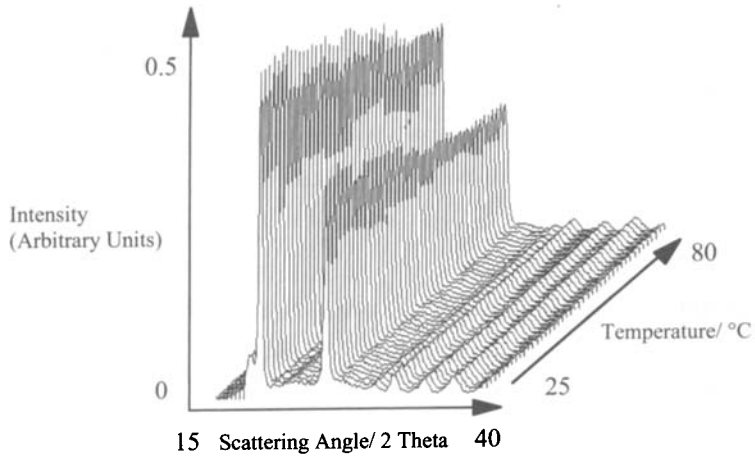

Figure 4: The dynamic WAXS intensity profile for the drying of PGA degraded for 63 days. Small changes to the peak positions and widths are observed.

the peaks and a third order polynomial fit was found to be satisfactory for the amorphous halo.

The positions of the (110) and (020) peaks were used to calculate the *a* and *b* dimensions of the unit cell. The unit cell dimensions show a small amount of thermal expansion as expected, although the changes are smaller than those due to sample variation, figure 5. The peak widths of the highly degraded samples increase with drying, but no corresponding change is seen in the sample degraded for 1 hour, figures 6 and 7. There is significant random variation in the peak widths from sample to sample, but the variation in a single sample as the temperature is raised is much smaller and the trends seen on dehydration can be believed. The high degree of instrumental broadening prevents quantitative analysis of these peak widths. However, since the instrumental broadening is constant throughout the experiment, again the trends are reliable.

TGA of samples dried using different techniques. The TGA results show a dramatic difference in the water content of degraded PGA depending on the method of sample preparation employed, figure 8. The fully hydrated sample shows a 4.2% weight loss after heating to 100°C. A 2.1% weight loss is seen in the sample desiccated then stored at 97% humidity for 2 hours. A 0.7% weight loss is seen in the desiccated sample, while only a 0.2% weight loss is seen in the vacuum dried sample.

SAXS of samples dried using different techniques. A comparison of the SAXS data for PGA degraded for 7, 14 and 28 days in the fully hydrated state, after freeze-drying and after vacuum drying is shown in figure 9. It is clear that drying changes the profile shape and that the different methods of drying do so in significantly different ways.

ESEM during dehydration. Figure 10 shows wet PGA, degraded for 28 days, showing a smooth almost featureless surface. Figure 11 illustrates the microstructure after slow removal of water and figure 12 after rapid removal of water. The rapidly dehydrated sample shows

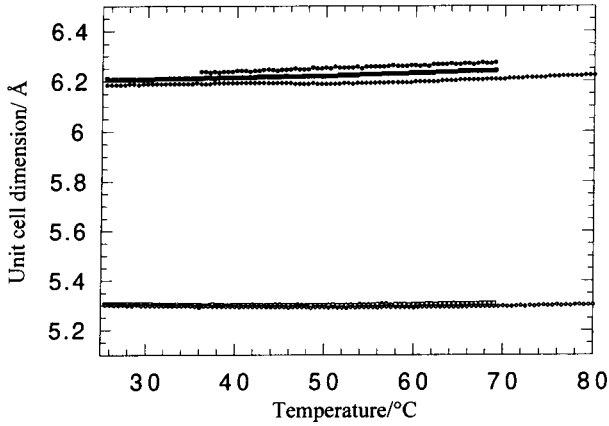

Figure 5: The *a* and *b* dimensions of the unit cell plotted against temperature for samples degraded for 1 hour (circles), 28 days (squares) and 63 days (diamonds). The *a* dimensions are denoted by open symbols and the *b* dimensions by closed symbols.

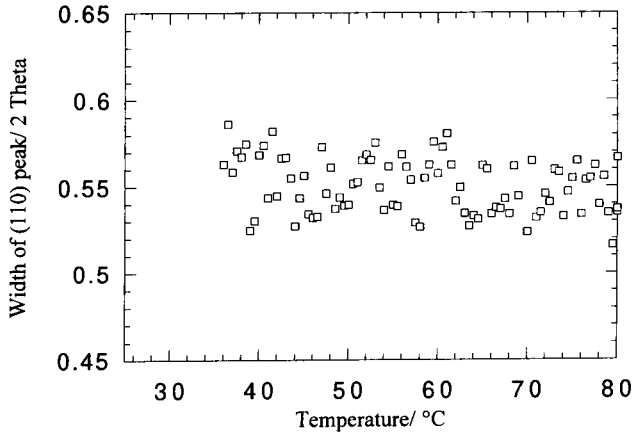

Fig.6a

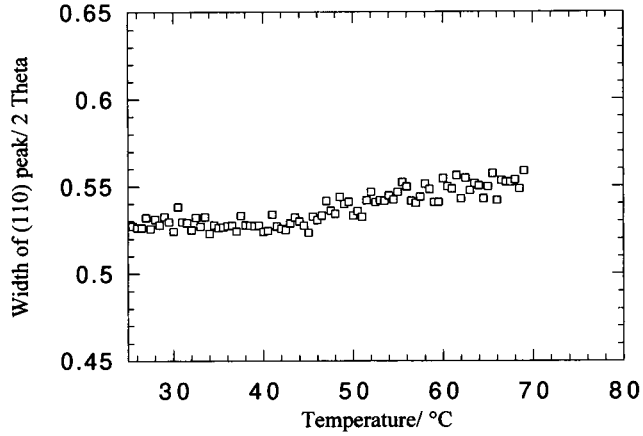

Fig. 6b

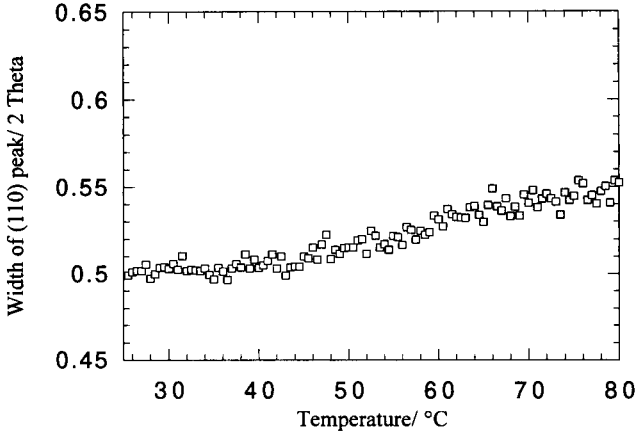

Fig. 6c

Figure 6: The width of the (110) peak plotted against temperature for samples degraded for a) 1 hour, b) 28 days and c) 63 days. There is significant random variation in the peak widths from sample to sample, but the random variation in a single sample as the temperature is raised is much smaller and the trends seen on dehydration can be believed.

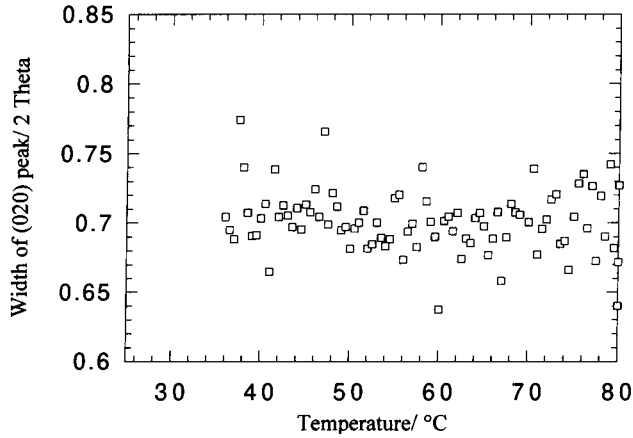

Fig. 7a

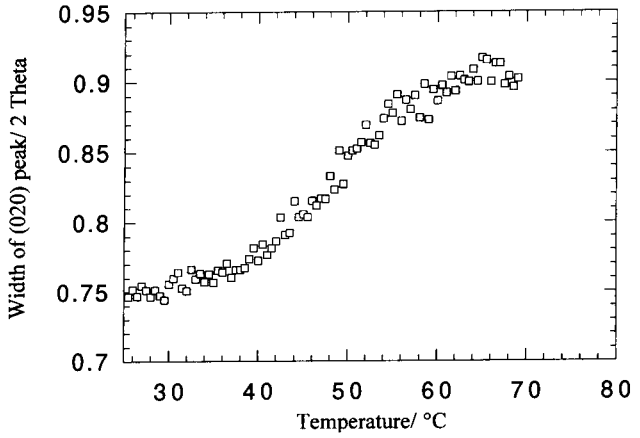

Fig. 7b

Figure 7: The width of the (020) peaks plotted against temperature for samples degraded for a) 1 hour, b) 28 days and c) 63 days. There is significant random variation in the peak widths from sample to sample, but the random variation in a single sample as the temperature is raised is much smaller and the trends seen on dehydration can be believed.

Fig. 7c

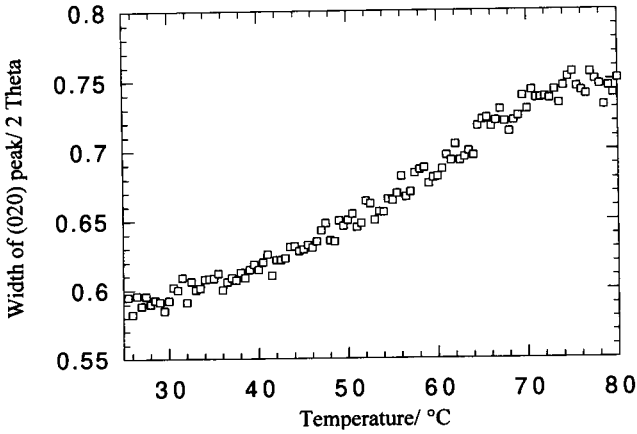

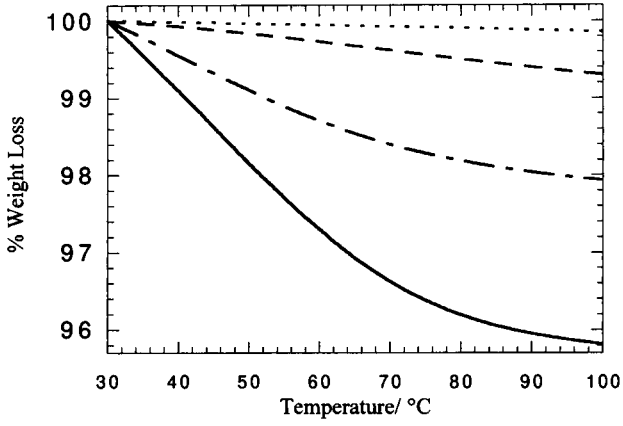

Figure 8: The TGA results of PGA degraded for 21 days then analysed wet (straight line), after vacuum desiccation (dashed line), after drying in a vacuum oven (dotted line) and after vacuum desiccation then storage at 97% humidity for 2 hours (dot/dash line).

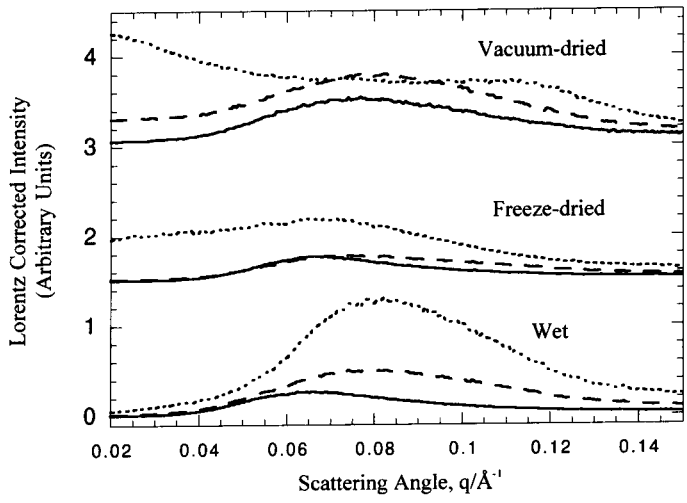

Figure 9: The SAXS intensity profile for samples degraded for 7 days (straight line), 14 days (dashed line) and 28 days (dotted line).The samples are observed wet, after freeze-drying and after vacuum-drying. The curves have been offset for clarity.

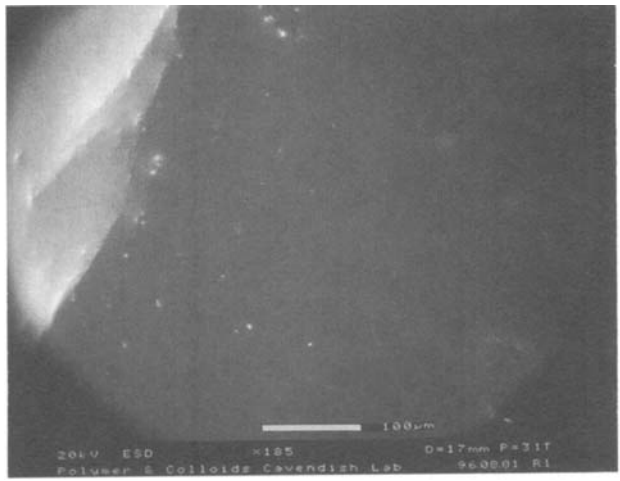

Figure 10: ESEM micrograph of wet PGA previously degraded for 28 days. The surface morphology is smooth and almost featureless.

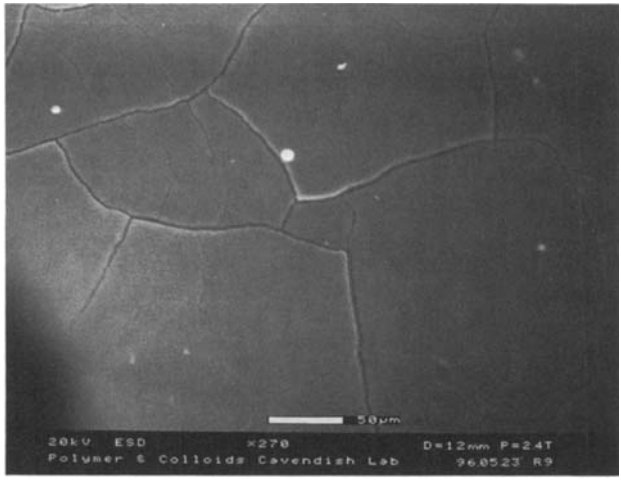

Figure 11: ESEM of wet PGA previously degraded for 28 days and slowly dried in the microscope chamber.

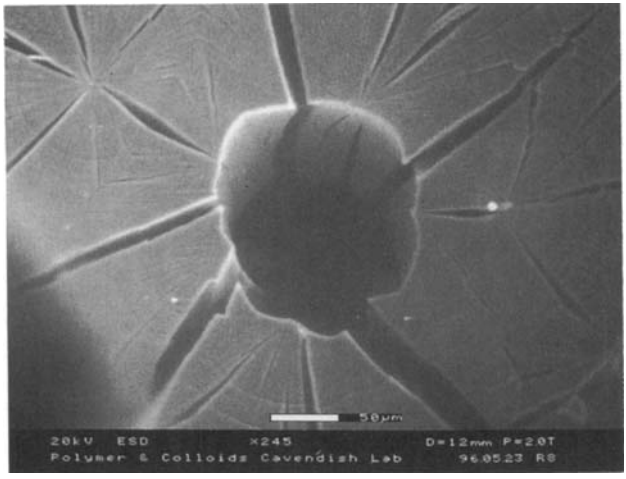

Figure 12: ESEM micrograph of wet PGA previously degraded for 28 days and rapidly dried in the microscope chamber. The cracks reflect the spherulitic morphology of the sample.

cracks are of varying size up to tens of microns in width. The voids appear to reflect the spherulitic morphology, with clear radial voids and some tangential features. The slowly degraded sample shows a system of narrower voids whose structure appears to be much less dominated by the spherulitic morphology.

DISCUSSION

Void free microstructure in wet samples. SAXS intensity profiles of wet all samples before dehydration show no evidence of void scatter, figure 1. Further, there are no voids visible on the surface of a degraded structure viewed in the wet state by ESEM, figure 10. Thus, we have seen no evidence of void structure in degraded and undegraded samples before dehydration.

Voiding and collapse of the lamellar structure. The SAXS profile from the sample degraded for only 1 hour exhibits little change on dehydration (figure 1a). However, the profiles from samples degraded for 28 and 63 days (figures 1b & 1c) show a large increase in intensity at low angles as dehydration proceeds. Such scattering is characteristic of void formation. The voids are large, since they scatter at small angles, and are probably of irregular size and spacing since the scattering is featureless.

On dehydration, the lamellar repeat distances for the samples degraded for 28 and 63 days decrease rapidly. This indicates a collapse of the lamellar structure accompanying the opening up of voids. In other words, as water is removed from degraded samples, the crystal lamellae move together lowering the overall spacing. This movement is possible since the degradation removed much of the amorphous phase between the crystals giving a more deformable structure [6, 7]. The complex spherulitic arrangement of lamellae does not allow the whole sample to shrink uniformly, so voids are opened elsewhere in the structure to relieve the internal stresses created by dehydration. No major changes are observed in the

sample degraded for 1 hour (figure 2). Since little or no amorphous material has been removed, the structure cannot respond to dehydration by lamellar collapse and voiding.

The invariant of PGA degraded for 1 hour increases slightly during dehydration (figure 3). In a non-voided two phase system, the invariant [12] may be represented by

$$Q = (\rho_c - \rho_a)^2 w_c(1-w_c) \qquad (2)$$

where ρ_c is the density of the crystalline material, ρ_a is the density of the amorphous material and w_c is the volume fraction of crystal. This model assumes sharp boundaries. (The addition of broad boundaries would introduce a small perturbation on this formula [12].) The increase in invariant in PGA degraded for 1 hour can be interpreted as being due to an increase in the first term. The removal of water increases the density difference between crystalline polymer and hydrated amorphous polymer compared with the density difference between crystalline polymer and dry amorphous polymer.

Before dehydration begins, there is little evidence of void scattering. The invariant is larger in more degraded samples because the interlamellar space has a lower density as amorphous polymer is replaced by buffer solution, so ρ_a is lower and the density difference is higher. We have discussed this in more detail elsewhere [6].

Once voids are introduced into the structure, it may no longer be assumed to be two phase and equation 2 no longer applies. Equation 3, gives the definition of invariant for a three phase structure with sharp boundaries, where ρ_o is the density of void, w_a is the volume fraction of amorphous material and w_o is the volume fraction of void [13].

$$Q = (\rho_c - \rho_a)^2 w_c w_a + (\rho_c - \rho_o)^2 w_c w_o + (\rho_a - \rho_o)^2 w_a w_o \qquad (3)$$

The invariant decreases on dehydration in the samples degraded for longer times. This effect is not straight forward to interpret because several factors are involved.

Firstly, the invariant is affected by decreasing long period of the structure as the lamellar structure collapses. As crystals move together, the density of the interlamellar space increases. This increases ρ_a and thus decreases ρ_c - ρ_a. The fraction of space occupied by the inter-lamellar space, w_a, also decreases. Both these effects decrease the invariant by way of the first term in equation 3.

However, hydration is also accompanied by the opening up of voids described by the second two terms in equation 3. The creation of empty voids introduces objects of very high contrast and would thus be expected to strongly *increase* the invariant. Given the high contrast of the voids, this effect would be expected to dominate.

The explanation for the decrease in invariant on dehydration may lie in the approximations made in its calculation. Strictly, the intensity should be integrated over the entire range of angles, from zero to infinity. In practice, data cannot be collected at very low angles due to the presence of the beam stop, or at high angles due to the end of the detector. If, as in this case, the invariant is calculated by integrating between the limits of data collection, only the scattering from objects of intermediate size is counted. Scattering from very large and very small objects does not, therefore contribute.

It is clear from figure 1 that the scattering at low angles increases dramatically during dehydration. It would seem that, as dehydration progresses, an increasing proportion of the scattering falls behind the beamstop and is not counted in the calculation of the invariant. The invariant decrease may thus be partly a consequence of the formation of voids that are very large and hence not seen in the SAXS due to the presence of the beam stop. Since these voided areas of the sample are not contributing to the observed scattering, the total scattering falls.

The invariant changes are thus consistent with collapse of the lamellar structure and voiding, but because of the competing contributions to it, further information cannot be gained.

It is instructive to compare the onset of the fall in the invariant and the long period, with the rise in scatter at low angles. As argued above, the increase in scatter at low angles probably represents only the smallest of the voids present. Larger voids appear behind the beam stop. Scattering at low angles appears immediately in the sample degraded for 28 days indicating that these small voids open up at once. In the sample degraded for 63 days, the low angle scatter does not appear until the final stages of dehydration, although the fall in long period and invariant begins immediately. This suggests that in the most degraded sample, large voids open and propagate easily with no need for smaller, energetically unfavourable voids until the final stages of dehydration. At earlier stages of degradation, the large voids meet more resistance to formation and both large and small voids appear at the beginning of dehydration.

Supporting evidence for the formation of large voids on drying is provided by the ESEM analysis. On drying the degraded PGA develops large cracks. These cracks would be much too large to scatter into SAXS regime measured by our experiment. Large radial voids are seen which are consistent with the voids opening as a consequence of lamellae collapsing together.

The extent of the damage is dramatically dependent on the rate of drying. The sample dried slowly (figure 11) exhibited relatively small surface cracking on drying, whereas the sample dried rapidly (figure 12) developed large surface cracks with extensive surface morphological damage. Presumably, in analogy with polymer deformation in response to stress, the higher the rate of dehydration, the less time there is for molecular relaxation to occur and hence the more extensive the void formation. These results indicate that the morphology of PGA is strongly affected by both degradation and drying, and that the rate of dehydration is an

important factor in the extent of the structural damage of samples where hydrolytic attack has occurred.

Freeze-drying after degradation does not prevent structural damage (figure 9). The degraded freeze-dried samples again show lamellar disruption due to the decrease in the lamellar repeat and the presence of voids. However, this damage, though still considerable, has less voiding and less collapse of the lamellar structure than the degraded material dried in a vacuum oven.

Crystal disruption. The widths of the (110) and (020) peaks for the 1 hour degraded PGA are unchanged by drying. However, the corresponding widths for the degraded samples increase on drying (figures, 6 and 7). Since the crystals are unlikely to decrease in size significantly during this treatment, these changes must reflect an increased disorder in the crystals. This is presumably the result of increased strain on the crystals as the lamellae collapse together and voids open simultaneously.

The increase the (020) width is greater than in the (110). A broadening of the (0*k*0) reflections in cold drawn and subsequently annealed PGA samples is reported by Chatani *et al*[5]. They hypothesised that the crystallites are easily distorted in the *b* direction by the migration of impurities or implied stress within the material.

The *a* and *b* dimensions of the unit cell increase in all samples as the temperature was increased (figure 5). These changes are presumably a consequence of thermal expansion. Similar results are seen in fully dried PGA [14] suggesting that neither degradation and dehydration have a significant effect on unit cell size or thermal expansion.

Water content. The TGA profile for the fully hydrated sample degraded for 21 days (figure 8) gives an indication of the extent of water loss during the dynamic X-ray experiments. It is clear from the profiles of dehydrated samples that even after harsh dehydration techniques PGA still retains a small amount of tightly bound water within its structure. The hydrophilic

nature of PGA is further demonstrated by the TGA profile of the sample dried then rehydrated at 97% humidity, the weight loss increasing from 0.7% to 2.1%.

Model for the dehydration of degraded PGA. The microstructural information described above is schematically illustrated in figure 13. After 1 hour degradation, the sample has undergone little hydrolytic attack and hence no significant changes to the microstructure occur on drying, figure 13a. After 28 days degradation, the sample is partially degraded, with some tie chains in the amorphous material still remaining. These provide some resistance to the formation of voids on dehydration. Thus, in this structure removal of water causes the lamellar structure to collapse slightly, small voids to form and crystallites to become strained, figure 13b. After 63 days degradation, most of the tie chains have been hydrolytically removed. This allows larger voids to form more readily on the removal of water. Only at later stages of dehydration do the smaller voids form, figure 13c. As before, these changes in microstructure are accompanied by increased strain in the crystallites.

There are clear parallels between voiding in degraded polymers during dehydration and crack propagation in polymers under stress. The nature of the material at the void (or crack) tip and the rate of dehydration (or deformation) play significant and comparable roles. This underlines the conclusion that dehydration of hydrolytically degraded PGA causes major damage to the microstructure.

CONCLUSIONS

Dehydration of hydrolytically degraded PGA structures causes significant microstructural change. On dehydration, the lamellae collapse together and voids open. The size of the voids is dependent on the extent of hydrolytic attack and is probably related to the number of remaining tie chains in the amorphous phase. The crystalline material becomes strained as the structure collapses. The extent of the morphological disruption caused by drying is dependent on the degree of degradation and on the rate and method of drying.

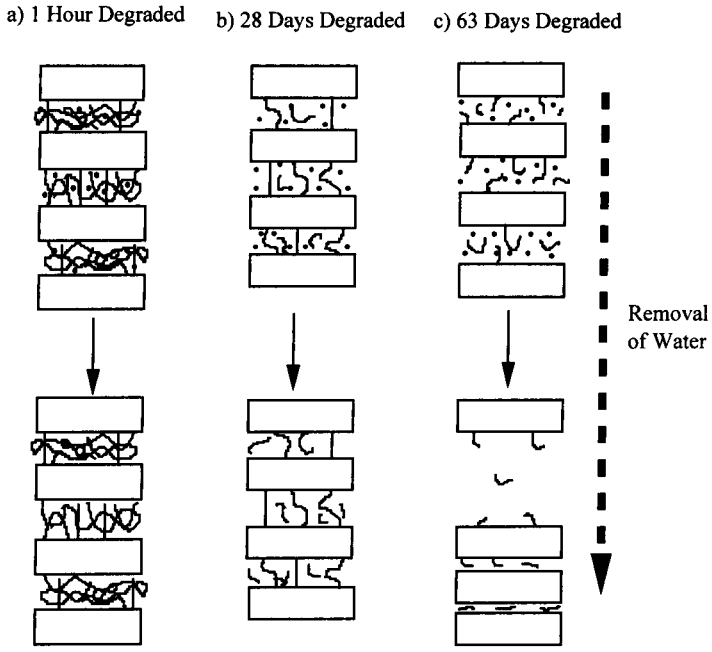

Figure 13: Schematic diagram of the changes that occur to the lamellar morphology of PGA on dehydration after previous degradation of a) 1 hour, b) 28 days and c) 63 days.

ACKNOWLEDGEMENTS

The authors are grateful to Pfizer Central Research and the EPSRC for financial support. The freeze-drying experiments were performed at Pfizer Central Research, Kent by Dr J. Richardson and Mrs J. Woods. The X-ray experiments were performed at the CCLRC Daresbury Laboratory with the help and advice of Dr B. U. Komanschek. The ESEM experiments were performed at the Cavendish Laboratory, University of Cambridge with the help of Mr. A. Eddie.

REFERENCES

1) X. Zhang, F. A. Goosen, U. P. Wyss & D. Pichora, Rev. Macromol. Chem. Phys., C33, 81 (1993).

2) C. C. Chu, J. Biomed. Mater. Res., 15, 19 (1981).

3) R. M. Ginde & R. K. Gupta, J. Appl. Polym. Sci., 33, 2411 (1987).

4) I. Engelberg & J. Kohn, Biomat., 12, 292 (1991).

5) Y. Chantani, K. Suehiro, Y. Okita, H. Tadokoro & K. Chujo., Makromol. Chem., 113, 215 (1968).

6) E. King & R. E. Cameron, To be published.

7) A. D'Emanuele, J. Kost, J. L. Hill & R. Langer, Macromol., 25, 511 (1992).

8) R. J. Ginde & R. K. Gupta, J. Appl. Polym. Sci., 33, 2411 (1987).

9) C. C. Chu, L. Zhang & L. D. Coyne, J. Appl. Polym. Sci., 56, 1275 (1995).

10) A. J. Ryan, S. Naylor, B. Komanschek, W. Bras, G. R. Mant & G. E. Derbyshire, ACS Symp., 581, 162 (1994).

11) R. E. Cameron, Trends in Polymer Science, 2, 116 (1994).

12) F. J. Balta & C. J. Vonk, Polymer Science Library 8:X-ray Scattering of Synthetic Polymers, Elsevier, Oxford (1989).

13) O. Glatter & O. Kratky, Small Angle X-ray Scattering, Academic Press, London (1982).

14) E. King & R. E. Cameron, To be published.